INL/CON-05-01001
PREPRINT

Insights From Laboratory Experiments On Simulated Faults With Application To Fracture Evolution In Geothermal Systems

41st U.S. Rock Mechanics Symposium - Golden Rocks 2006

S. L. Karner

June 2006

The INL is a
U.S. Department of Energy
National Laboratory
operated by
Battelle Energy Alliance

Insights from laboratory experiments on simulated faults with application to fracture evolution in geothermal systems

Karner, S. L.
Idaho National Laboratory, Idaho Falls, ID, USA
(now at: ExxonMobil Upstream Research Company, Houston, TX, USA)

ABSTRACT: Laboratory experiments provide a wealth of information related to mechanics of fracture initiation, fracture propagation processes, factors influencing fault strength, and spatio-temporal evolution of fracture properties. Much of the existing literature reports on laboratory studies involving a coupling of thermal, hydraulic, mechanical, and/or chemical processes. As these processes operate within subsurface environments exploited for their energy resource, laboratory results provide insights into factors influencing the mechanical and hydraulic properties of geothermal systems. I report on laboratory observations of strength and fluid transport properties during deformation of simulated faults. The results show systematic trends that vary with stress state, deformation rate, thermal conditions, fluid content, and rock composition. When related to geophysical and geologic measurements obtained from engineered geothermal systems (e.g. microseismicity, wellbore studies, tracer analysis), laboratory results provide a means by which the evolving thermal reservoir can be interpreted in terms of physico-chemical processes. For example, estimates of energy release and microearthquake locations from seismic moment tensor analysis can be related to strength variations observed from friction experiments. Such correlations between laboratory and field data allow for better interpretations about the evolving mechanical and fluid transport properties in the geothermal reservoir – ultimately leading to improvements in managing the resource.

1. INTRODUCTION

Successful energy extraction from the vast subsurface thermal resource requires a thorough understanding of the generation and maintenance of permeable pathways. As a majority of geothermal reservoirs are comprised of igneous and metamorphic rocks with low matrix permeability, the pathways for fluid-flow inherently involve a network of interlinked cracks and fractures. Where such a pathway does not exist, or is inadequate for economic energy production, then the permeable fracture network needs to be engineered by creating new fractures or inducing shear on pre-existing fractures. Furthermore, the quality of the permeable network will need to be monitored and adjusted over time in order to properly manage the thermal resource during the several decade lifespan of an exploitable geothermal field.

Results from laboratory experiments are invaluable for helping understand the complexities of the processes that operate within the Earth. Of particular relevance for engineered geothermal systems are concepts stemming from experiments that explore the mechanics of fracture generation [e.g. 1-8], physical factors controlling the strength of existing fractures [e.g. 9-15], the effects of fluid-rock interactions on strength properties [e.g. 16-22], and permeability evolution within the fracture network [e.g. 21-26]. The salient details from existing laboratory studies that explore these effects are presented here, with a focus on implications for successful exploitation of fractured geothermal systems.

2. FRACTURE GENERATION

The primary process by which the permeability of engineered geothermal systems is improved is via subsurface hydraulic fracturing initiated from a wellbore. The premise of hydraulic fracturing is that a working fluid is pumped downhole to pressures exceeding the in-situ stress field and strength of the rock in order to generate crack networks. The planes of the hydraulically induced fractures that emanate from the borehole are typically thought to be oriented perpendicular to the minimum compressive stress in the subsurface. This assumption can be used, in turn, to determine the orientation and the amplitude of the in-situ stress field via small scale hydraulic fracturing (i.e. mini-fracs). However, recent laboratory data illustrates aspects of the Mohr-Coulomb failure envelopes for rocks that complicates the simple assumption used above.

Ramsey and Chester [15] performed room temperature, room humidity extension experiments on necked (dogbone) samples of Cararra Marble to explore the transition from tensile cracks (Mode I) to the generation of shear fractures (Mode II or III). They explored failure characteristics for a range of confining pressures and observed a systematic change in fracture style and material strength (Figure 1). At low confining pressures, samples failed under extensional stress conditions with tensile strengths compatible with those of previous studies. The through-going fractures associated with sample failure display orientations that are nearly normal to the direction of the minimum stress. At high confining pressures, samples failed with compressive minimum stresses and the extensional fractures form at lower angles to the minimum stress direction (less than ~75^o). Further, the high confining pressure fractures have displacements and surface morphologies consistent with opening mode shear fractures. Similar results have been reported for Berea Sandstone [27], indicating that these trends may be observed for a variety of rock types – yet, the stress values may vary. The results from these experiments are wholly consistent with expectations of fracture angles calculated from the low stress portion of the Mohr-Coulomb failure envelope (see [28] for a discussion of failure envelopes and methods to perform these calculations).

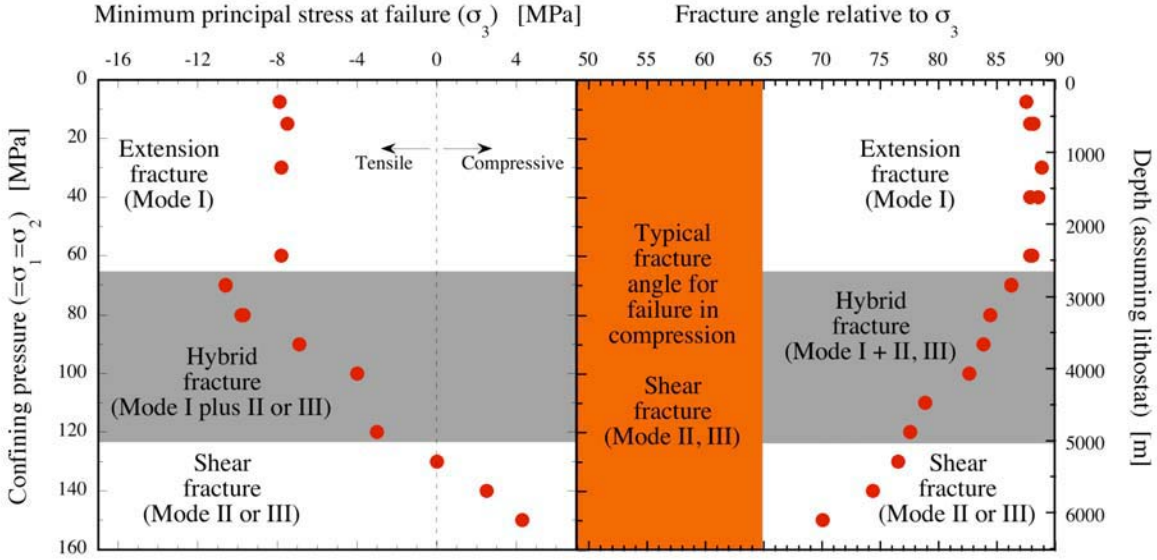

Fig. 1. Results from failure experiments on necked (dog-bone) samples of Cararra Marble (modified from [15]). For all experiments, samples were subjected to tensile strain leading to failure with the minimum and maximum stresses at failure recorded for each experiment. Failure stresses are plotted in the left subplot, with the maximum compressive stress (confining pressure) equated to depth by assuming a normal faulting stress regime (vertical stress is the maximum stress) and a lithostatic gradient of ~24.5 MPa/km. The minimum compressive stress at failure transitions from tensile to compressive as a function of increasing confining pressure (or depth) and delineates the low stress portion of the failure envelope for Cararra Marble. The observed fracture orientation relative to σ_3 systematically decreases with increasing confining pressure. Similar results have been reported from identical tests on Berea Sandstone [27].

While Cararra Marble or Berea Sandstone are not the best proxies for geothermal reservoir rocks, a comparison of mechanical properties for geothermal rocks (e.g. granite) to in-situ stresses indicates that the transition in fracture angle observed by Ramsey and Chester [15] may be important (particularly as deeper reservoirs are tapped as an energy source).

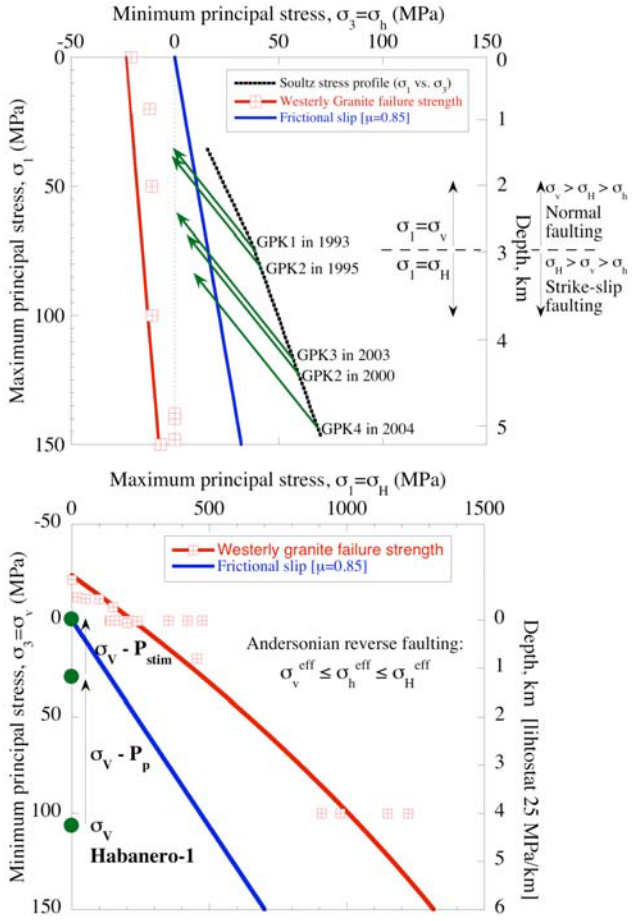

Fig. 2. Analysis of stimulation at Soultz-sous-Fôrets, France (top) and Habanero-1 in the Cooper Basin, Australia (bottom). Downhole crustal stress data and hydraulic stimulation pressures are compared to laboratory data (square symbols, with polynomial curve-fit) for room-temperature fracture strength of Westerly Granite [16, 29-30] and the frictional strength envelope for a cohesionless fracture (μ=0.85). **a)** Data from Soultz-sous-Fôrets, France. Stress-profile for Soultz (heavy dotted line) and stimulation fluid pressures are from [31]. Horizontal direction is least compressive stress (σ_h). Direction of the maximum compressive stress changes with depth, showing normal faulting at shallow levels and strike-slip at deeper levels. Stimulation data are used to calculate effective stresses at failure (diagonal lines). **b)** Data from Habanero-1 well in the Cooper Basin, Australia [see 32 for details]. Vertical direction is least compressive stress (σ_v). In-situ fluid pressure (P_p) and stimulation fluid pressure (P_{stim}) are used to calculate effective pressure at depth (solid circles). Assuming reverse faulting, failure of intact granite requires a horizontal stress ~200 MPa greater than the value of the vertical stress.

It is important to recognize that the Earth is typically not in a pristine undeformed state. For example, geothermal reservoirs contain abundant joints, cracks, fractures, and faults that can be exploited during stimulation. These pre-existing features require lower fluid pressures to overcome cohesion compared to pressures needed to fracture undeformed rock (Figure 2). As these frictional surfaces also play a major role in the development of exploitable geothermal systems, it is important to consider laboratory tests that explore the factors that influence frictional strength of simulated fractures.

3. MECHANICAL EVOLUTION OF FRACTURES

Concern over fractures in geothermal systems does not end with the successful generation of an interconnected network. When hydraulic stimulation involves pre-existing fractures, an anisotropic stress field, or certain rock properties, the stimulated fractures may experience some portion of the total deformation in the form of shear displacement. The shearing may be contemporaneous with the stimulation process itself, but will likely include a protracted stage of creep following stimulation. The shearing of the fracture and associated creep not only serve to lower porosity and permeability, but will also increase the cohesive strength of the fracture. From a mechanical perspective, the material that comprises asperities within fractures will deform due to the applied normal and /or shear loads. Should this deformation occur over a period of time then the real area of contact between the fracture walls will increase. As real area of contact and cohesion are considered to be the primary factors defining fracture strength [10-11, 33], then the frictional behavior of fractures should evolve with mechanical loads and time.

3.1. Time dependence

The time-dependent strengthening (or aging) of a fracture is exemplified by results from frictional slide-hold-slide experiments on shear zones that may or may not contain wear material (Fig. 3; for a review see [34]). In these tests, shear zones are deformed at a constant sliding rate (slide) with episodic intervals for which the imposed loading rate is set to zero (hold). During the hold interval, the shear zone supports a residual shear stress that decays exponentially with time due to frictional creep (Fig. 3a). On reloading after a hold (slide),

the frictional resistance increases to a peak value and subsequently approaches the steady-state sliding value. As the reloading peak is considered to be a measure of static friction levels, then the difference between the peak friction and the steady-state sliding friction level provides a measure of restrengthening (healing). Laboratory slide-hold-slide tests consistently show that frictional strength increases logarithmically with stationary hold time (Fig. 3b). For bare sliding surfaces (with no wear material, or gouge), the time-dependent healing is associated with growth of asperity contacts and an increase in adhesion [e.g. 34]. When sand layers are sheared (simulating gouge), the healing is associated with compaction (or densification) of the layer (Fig. 3c), consistent with the notion that frictional healing is due to time-dependent increase in real area of contact [e.g. 10].

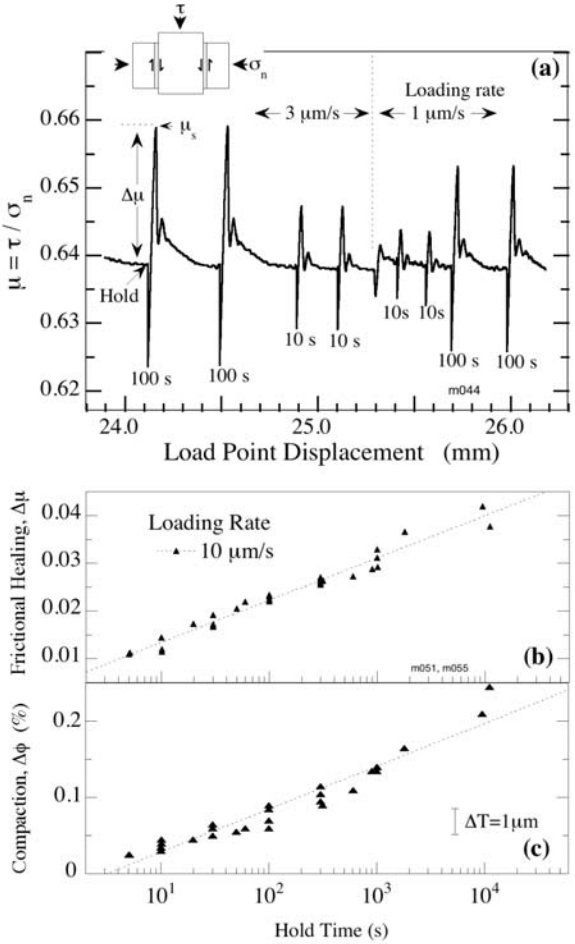

Fig. 3. Results from slide-hold-slide shear tests in quartz sand (modified from [37]). Holds start when loading rate is set to zero. In holds, stress-relaxation occurs (Fig. 3a) with compaction of the layer (Fig. 3c). Friction restrengthening occurs on reloading (Δμ; Fig. 3a) and this scales with the logarithm of hold time (Fig. 3b). Identical time-dependent behavior has been noted during stable shear on bare surfaces.

Several constitutive relations have been derived to mathematically describe the rate- and state-dependent behavior of rock friction. The two most widely used friction relations are: 1) the time-dependent (or slowness) law, which I refer to as the Dieterich law [35], and 2) the slip-dependent law, which I refer to as the Ruina law [36]. These relations are similar in that they describe time and velocity dependence of friction (μ) by the relation:

$$\frac{\tau}{\sigma_n} = \mu = \mu_0 + a\ln\left(\frac{V}{V_0}\right) + b\ln\left(\frac{V_0\theta}{D_c}\right) \qquad (1)$$

Here μ_0 represents steady-state friction for slip at a reference velocity, V_0, where V is the sliding velocity, D_c is a critical slip distance, θ is a state variable, a and b are scaling constants, τ is shear stress and σ_n is normal stress. However, the similarity between these relations does not extend to their description of evolution of the state variable. The Dieterich evolution law [35]:

$$\frac{d\theta}{dt} = 1 - \left(\frac{V\theta}{D_c}\right) \qquad (2a)$$

permits state evolution for frictional surfaces held in true stationary contact (V=0), whereas the Ruina evolution law [36]

$$\frac{d\theta}{dt} = -\frac{V\theta}{D_c}\ln\left(\frac{V\theta}{D_c}\right) \qquad (2b)$$

requires some finite slip for the state to evolve. In applying these relations to laboratory data, equations 1-2 must be coupled with a relation describing elastic interaction with the loading apparatus: $d\mu/dt = k\,(V_L - V)$, where V_L is the loading velocity prior to a hold, and k is a measure of apparatus stiffness.

The Dieterich and Ruina laws are capable of describing a variety of friction observations from laboratory experiments, despite their different descriptions of state evolution. Several studies have shown that friction may evolve in a more complex manner than described by existing constitutive relations, such as for large changes in shear stress [13, 37-39], or large variations in normal stress [12, 40-41]. Despite these complexities, the widespread applicability of the rate- and state-dependent friction relations make them a potentially valuable tool for modeling the strength evolution of fractures in geothermal systems.

3.2. *Normal stress effects*

By its very definition, friction is dependent on both the amplitude of the applied normal stress and the shear load required to initiate slip. However, the results from several studies show that friction evolves in a more complex manner when responding to large changes in shear stress [13, 37-39] or large variations in normal stress [12, 40-41].

For steady-state sliding at a reference friction level, any step-change in normal stress is typically countered by a similar change in shear stress so as to re-establish the reference friction level. However, recent laboratory results indicate that the amplitude of shear stress response ($\Delta\tau$) not only scales with the new normal stress level (σ_{final}) but also scales logarithmically with the ratio of new normal stress to the old normal stress (σ_0) [12, 40]:

$$\Delta\tau = k\sigma_{final} \ln\left(\frac{\sigma_{final}}{\sigma_0}\right) \qquad (3)$$

Additional complexities arise when normal stress is cyclically varied during the hold intervals of slide-hold-slide tests on simulated fault gouge [40]. For gouge layers, the cyclic vibration of normal stress during holds serves to densify the granular layer and to enhance the amount of stress relaxation. Upon reload after holds, shear stress increases to greater levels than observed without the vibrations (i.e. there is more healing). The amount of stress relaxation in holds and healing on reload scales with the amplitude of the normal stress vibrations. Furthermore, healing rates (e.g. Figure 3b) are also enhanced by vibrating the normal stress in holds.

These effects may translate to engineered geothermal systems inasmuch as cyclic variations in effective normal stress are often induced during hydraulic pumping. However, while similar normal stress dependent trends might be observed for deformation of bare sliding surfaces such a parametric laboratory study has yet to be done.

3.3. *Shear stress effects*

The influence of large variations in shear stress has been studied for simulated fault gouge [37-39] and bare surfaces [13]. These studies employ a modified form of the slide-hold-slide technique described earlier. For these tests, shear load is rapidly changed from the prehold sliding level τ_{slide} to a reduced level for holds τ_{hold}. Healing is studied as a function of shear load during the holds (τ_{hold}/τ_{slide} from 0 to 1; Figure 4) and hold time (to 10000 s).

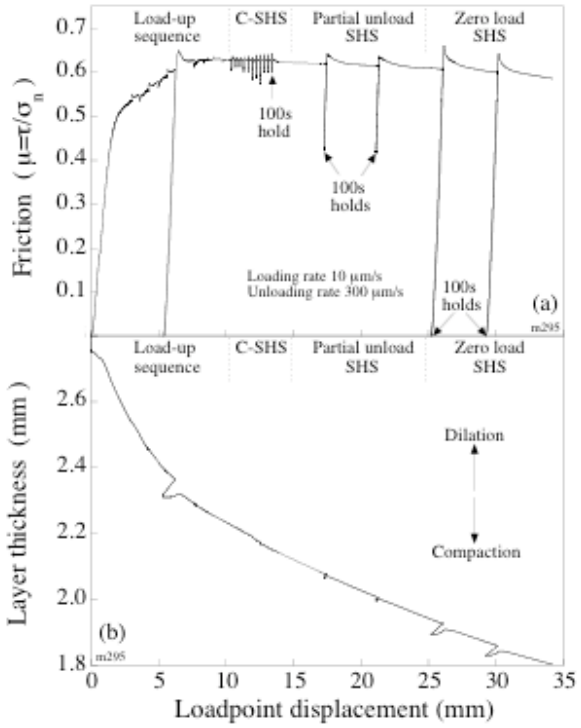

Fig. 4. Data from one test on simulated gouge involving holds at different shear loads [after 39]. (a) Friction is shown against load point displacement. Base level sliding friction decreases slightly with slip. Data show a set of CSHS tests with hold times between 10 and 10000 s. The last three hold cycles were of 100 s duration. For comparison, the next two hold cycles (100 s) were performed at a reduced shear load ($\mu_{hold} \sim 0.4$), and the last two hold cycles involved complete removal of shear load. Peak static yield strength increases as τ_{hold} decreases. (b) Layer thickness data are shown for the same test in Figure 4a. Layers thin with increasing shear displacement. Layer thickness variations are larger for holds with lower levels of τ_{hold}.

The results show systematic variations in healing and healing rates as a function of these variables (Figs. 5 and 6). For simulated gouge layers, the amplitude of healing increases as a function of greater reduction in shear stress for holds (Figs. 5a, 6a). However, bare surfaces show the opposite trend with healing levels decreasing dramatically as shear load for holds approaches zero. The time-dependence of healing when holds are performed at or near zero shear load also varies according to the nature of the shear zone (Figs. 5b, 6b). For zero-load during holds, healing rates for gouge are slightly negative (time-dependent weakening) whereas the rates for bare surfaces are positive (time-dependent strengthening). For both gouge and bare surfaces, healing rates decrease with lower shear stress during holds, with gouge healing rates transitioning from being positive (strengthening) to negative (weakening).

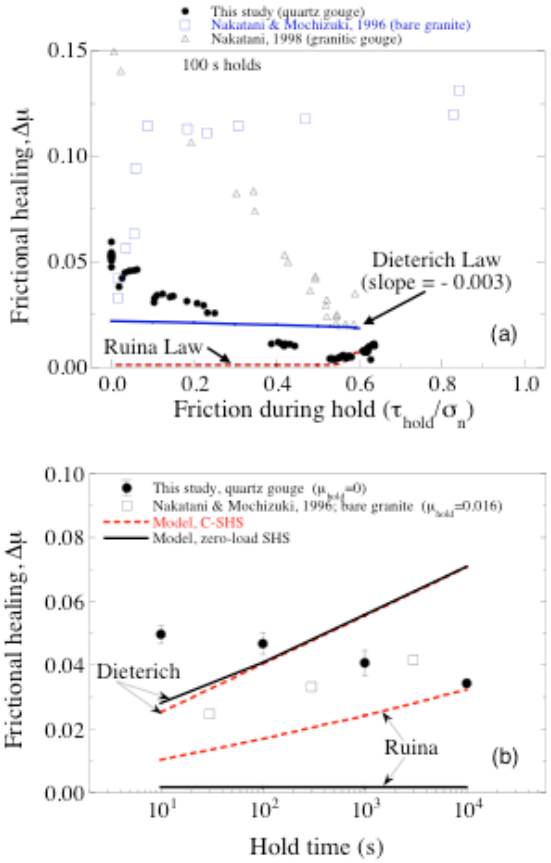

Fig. 5. Results from shear experiments on simulated gouge [37-39] are compared to bare surface friction [13] together with healing predicted by the Dieterich and Ruina friction relations (Eq. 1-2) [after 39]. For simulations, friction parameters were determined from velocity steps in the tests (a = 0.0066, b = 0.0066, and D_c = 45 μm). (a) Data from 100 s holds show lower healing levels and an inverse load dependence compared to data from bare granite surfaces. Neither of the friction relations satisfactorily describe the data. (b) Mean values of zero-load data for gouge [39] are compared to results from bare surface shear tests [13] together with healing predictions for regular slide-hold-slide tests (e.g. Fig. 3) and zero-load tests. For total shear load reduction during holds, gouge layers exhibit time-dependent weakening whereas bare surface shows time-dependent strengthening. Neither the absolute value of healing nor the time dependence are well matched by rate-state model predictions.

Neither the load nor time dependent characteristics are well modeled by existing rate and state friction relations, suggesting that these formulations are best suited to describe deformation close to steady-state sliding levels. It may be possible that an extended friction relation that accounts for volumetric deformation in three dimensions could describe these data [e.g. 42-43]. At present, however, this requires investigation and further study.

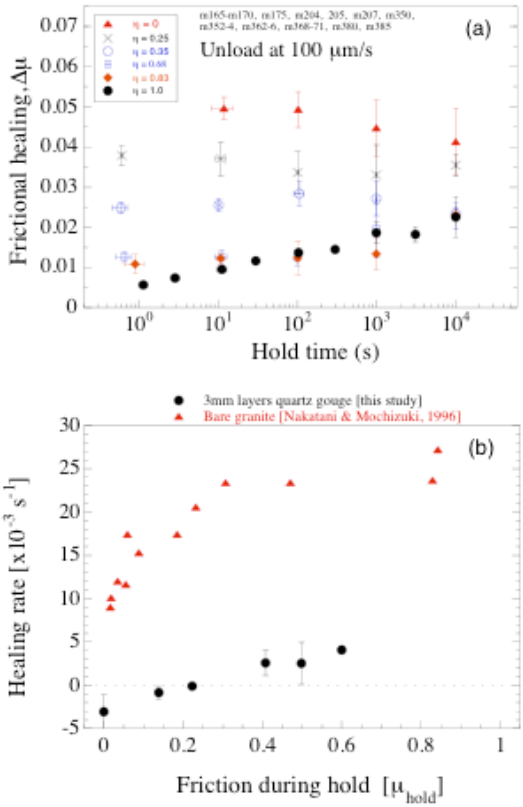

Fig. 6. Healing data from tests on gouge at different levels of shear stress for holds (η) are shown as a function of hold time [after 39]. (a) Mean healing values (symbols) are shown with standard deviation (bars). Healing systematically decreases with increasing hold shear stress. Note the systematic transition in healing rates from time-dependent weakening (η = 0) to time-dependent strengthening (η = 1). (b) Healing rates β expressed as $\Delta\mu x10^{-3}$ per decade time (in seconds) were obtained from the tests plotted in Figure 5a, with bars indicating error (in terms of correlation coefficient, 1-R). The results indicate that healing rate increases quasi-linearly with increasing η.

The influence of large shear stress perturbations may be very important for energy exploitation in geothermal systems. For example, during hydraulic simulation a large number of microseismic events are recorded (in the thousands). A majority of these events occur via shear failure and are presumably associated with a reduction in shear stress. If the reduction in shear stress is significant, then the temporal evolution of the fractures should display similar character to the laboratory observations reported above. This will be important for the long-term management of the fracture network, with particular relevance if restimulation is necessary. Furthermore, by coupling the seismic estimates of stress drop to the laboratory observations it may be possible to derive mechanistic interpretations regarding evolution of the fracture network.

4. FLUID-ROCK INTERACTIONS

The discussions in the previous sections highlight important aspects of geomechanical properties that can be studied from laboratory experiments. However, the results described above were all obtained from room-temperature tests and, therefore, may not provide a complete description for strength evolution in geothermal systems. While fractures can obtain greater adhesion (hence, strength) via mechanical deformation of contacting asperities, fracture strength can also be influenced by pressure solution of contacting asperities or by diagenetic precipitation of cements bonding fracture walls together [e.g. 17-22]. Also, the permeability of porous media has been observed to vary as hydrothermal diagenesis proceeds [22, 44]. The time-dependent character of strength and permeability under hydrothermal conditions is primaril due to the fact that geochemical reactions are rate-dependent.

At low temperatures (less than ~400^{o}C), the strength of aqueous silicate-bearing shear zones (i.e. quartz, feldspar) generally increases with longer reaction time [18-20] while the permeability typically decreases [21-22]. At high temperatures (greater than ~400 ^{o}C), silicate shear zones may show little to no time evolution in strength [18-20] and permeability reduction may be enhanced. However, it is important to note that these generalizations may not be universal. For example, common by-products from low temperature diagenesis are clays – which have been shown to dramatically reduce frictional strength of shear zones [e.g. 34]. Thus, the temporal evolution of strength, porosity, and permeability of fractures in geothermal systems will likely be determined by a variety of site-specific properties (e.g. physico-chemical environment, lithology and/or mineralogy, fluid composition).

Chemical reaction rates are typically too slow to explore the petrophysical and geomechanical evolution of fractures from hydrothermal laboratory experiments because the exposed surface area of fractures is comparatively small. Reaction rates can be enhanced if the fluid-rock surface area is increased. Thus, the large surface area of pore space in granular aggregates make them ideal materials to study the temporal evolution of rock properties at laboratory hydrothermal conditions.

It is commonly assumed that the extent of lithification in granular media increases with temperature and time. It is also assumed that lithification generally acts to increase the strength of a granular media. Indeed, the peak strength of water-saturated granular quartz powder (simulating fault gouge) does vary systematically with both temperature and time [19]. The peak strength of quartz gouge increases quasi-linearly with temperature (to 800^{o}C). Yet, the temporal evolution of the fault strength does not appear to be as straightforward.

Hydrothermal shear experiments can be used to constrain restrengthening models. Previous works have reported results from layers of powdered quartz subjected to slide-hold-slide tests performed at a range of temperatures [18-20]. The rate and state friction parameters (a, b, D_c from the friction constitutive relation shown in Eq. 1-2) were determined from data inversion using a Levenberg-Marquardt method (Fig. 7a; see [45] for details) and the values from [18-20] are shown in Table 2. These parameters are important for friction analyses as they help constrain fault rupture models and slip patch source properties. Of particular note here is that the difference between the two friction coefficients (i.e. a and b from Eq. 2) can be compared to previous results used to determine frictional stability ([20], see Fig. 7b). Negative values of (a-b) indicate that a material is prone to seismic instability (velocity-weakening, between 50-350 ^{o}C in Fig. 7b) and that materials with positive values are always stable.

Table 1. Rate and state friction parameters derived from numerical inversion of hydrothermal experiments on quartz powder layers [18-20]. Except for the highest temperature, inversions were performed using a two state-variable Dieterich model with the associated parameters indicated by subscripts.

Temperature	a	b_1	Dc_1 (μm)	b_1	Dc_2(μm)
250 ^{o}C	0.006	0.005	6.5	0.003	647.7
350 ^{o}C	0.005	0.005	4.4	-0.002	32.6
450 ^{o}C	0.052	0.003	3.3	-0.034	5845.8
600, 636 ^{o}C	0.016	-0.048	324.1	--	--

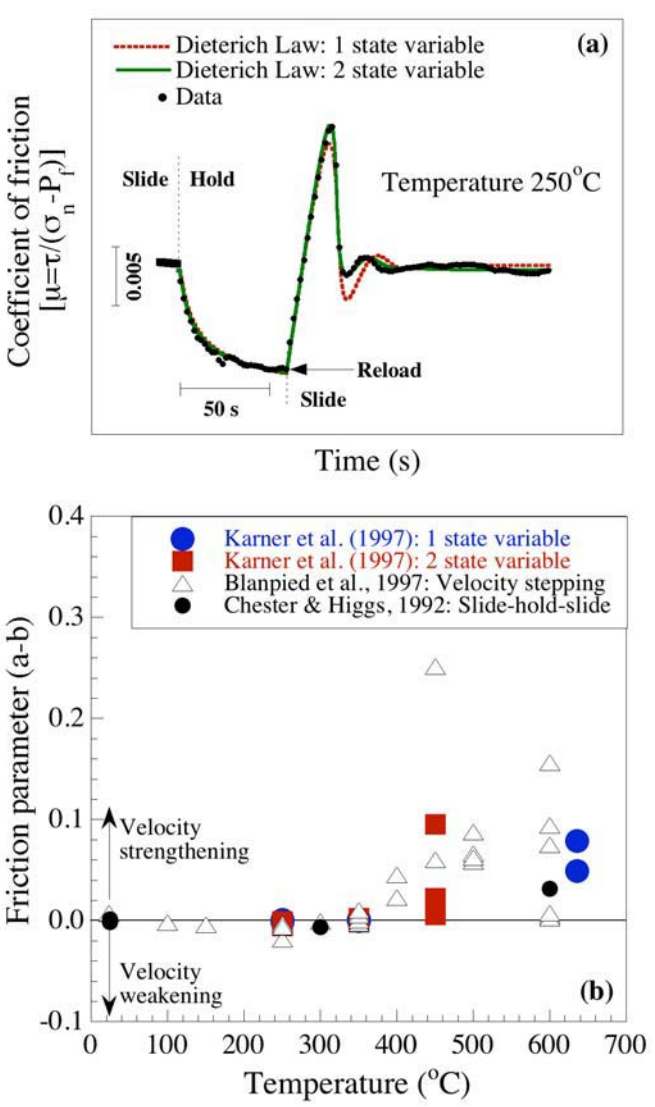

Fig. 7. Results from slide-hold-slide tests in layers of powdered quartz sand [19] performed in a triaxial shear apparatus (Fig. 5a). a). The rate and state friction parameters (a, b, D_c in Eq. 1-2) were obtained from inversion of experiment data. For tests at a given temperature, the results from inversions using the Dieterich formulation were averaged and these are shown in Table 1. b). The difference between the friction parameters a and b are used to identify the conditions at which frictional instability may occur. Stability analyses of the hydrothermal slide-hold-slide tests presented here (for quartz powder layers) are consistent with both previous work on granite [20] and quartz sand [18].

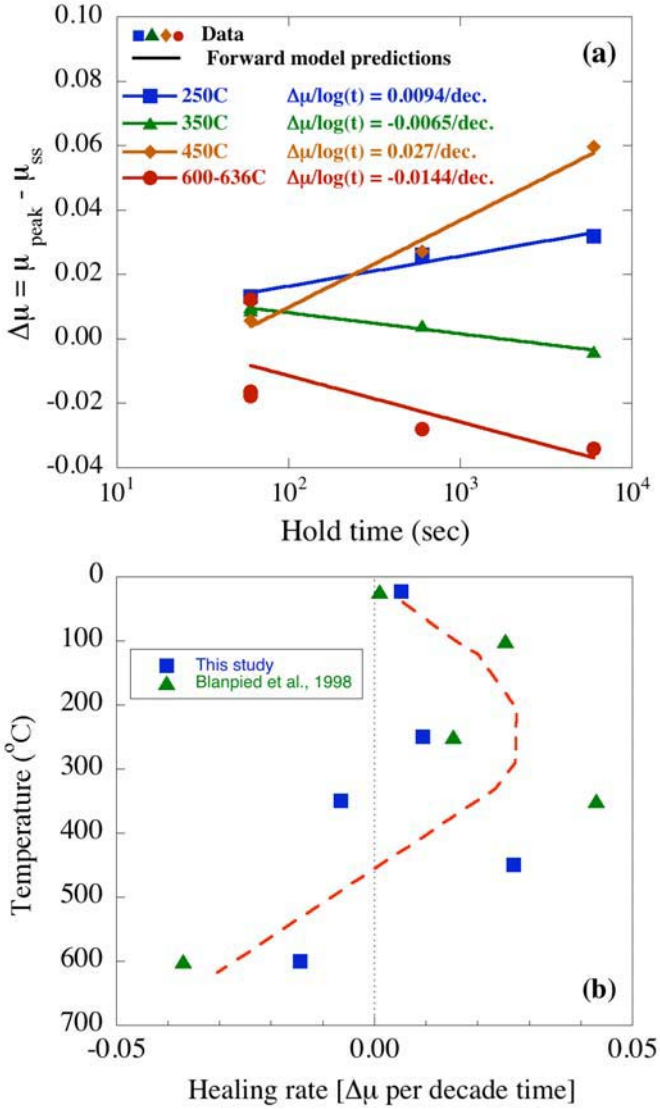

Fig. 8. Predictions of fault healing compared to the slide-hold-slide data shown previously in Figs. 3-6. a). Data for layers of quartz powder are well matched by the numerical predictions using the parameters shown in Table 1. b). The healing predictions shown in (a) are coupled with room-temperature healing data for quartz gouge (e.g. Fig. 3) and healing predicted from friction parameters derived for shear of granitic gouge [20]. Temperature is plotted as the vertical axis as a proxy for depth within the crust. The compilation of data indicate that healing rates vary as a function of temperature (or depth) with a transition to negative healing rates at very high temperatures (>500 °C). These results indicate that fractures in geothermal systems (T<350 °C) will tend to regain strength with time.

The friction parameters obtained from data inversion can also be used in forward models using the Dieterich friction evolution law (Eqs. 1-2a) to predict hydrothermal healing rates (see Fig. 7). The calculations provide a good match to observed data and indicate healing rates vary with temperature (Fig. 7a). Further, the results suggest that healing rates systematically decrease with increasing temperature, possibly due to thermally activated processes that enhance creep within the shear zone.

While the thermal conditions for these tests exceed those typically observed in geothermal systems, these laboratory results illustrate that temporal evolution of fracture strength can vary significantly with temperature. For typical geothermal fields (i.e. T<350 °C), the laboratory results also indicate that fractures embedded in silicate rocks (e.g. granites) will be conditionally unstable (velocity-weakening

part of Fig. 6b) and display positive restrengthening rates with time (Fig. 7). When coupled with moment tensor analyses derived from induced seismicity, the laboratory results offer mechanistic interpretations that may enable predictive modeling of strength evolution and propagation of fractures. These aspects are fundamentally important when fracture networks in geothermal fields are expected to be sustained for a considerable amount of time.

5. SUMMARY

I have summarized details from a series of experiments having relevance to the physical, chemical, and thermal conditions found in exploitable geothermal systems. The results show systematic trends that vary with stress state, deformation rate, thermal conditions, fluid content, and rock composition. When related to geophysical and geologic measurements obtained from engineered geothermal systems (e.g. microseismicity, wellbore studies, tracer analysis), laboratory results provide a means by which the evolving thermal reservoir can be interpreted in terms of physico-chemical processes.

6. ACKNOWLEDGEMENTS

This work was supported by the U.S. Department of Energy, Assistant Secretary for Energy Efficiency and Renewable Energy, Office of Geothermal Technology, under DOE Idaho Operations Office Contract DE-AC07-05ID14517, whose support is gratefully acknowledged

REFERENCES

1. Brace, W.F. 1960. An extension of the Griffith theory of fracture to rocks. *J. Geophys. Res.* 65: 3477-3480.
2. Brace, W.F. and E.G. Bombolakis. 1963. A note on brittle crack growth in compression. *J. Geophys. Res.* 68: 3709-3713.
3. Walsh, J.B. and W.F. Brace. 1964. Fracture criterion for brittle anisotropic rock. *J. Geophys. Res.* 69: 3449-3456.
4. Atkinson, B.K. 1980. Stress corrosion and the rate-dependent tensile failure of a fine-grained quartz rock, *Tectonophys.* 65: 281-290.
5. Costin, L.S. 1983. A microcrack model for the deformation and failure of brittle rock. *J. Geophys. Res.* 88: 9485-9492.
6. Costin, L.S. 1987. Time-dependant deformation and failure. In *Fracture Mechanics of Rock*, Academic Press, 167-215.
7. Lockner, D.A., J.D. Byerlee, V. Kuksenko, A. Ponomarev, and A. Sidorin. 1991. Quasi-static fault growth and shear fracture energy in granite. *Nature* 350: 39-42.
8. Engelder, T. 1994. Brittle crack propagation. In *Continental Deformation*, ed. P. L. Hancock, Pergamon Press, 43-52.
9. Logan, J.M. and J. Handin. 1971. Triaxial compression testing at intermediate strain rates. In *Dynamic Rock Mechanics*, 12th Symposium Rock Mechanics AIME, New York, 167 pp.
10. Dieterich, J.H. 1972. Time dependent friction in rocks. *J. Geophys. Res.* 77: 3691-3697.
11. Dieterich, J.H. 1978. Time dependent friction and the mechanics of stick-slip. *Pure Appl. Geophys.* 116: 790-805.
12. Linker, M.F. and J.H. Dieterich. 1992. Effects of variable normal stress on rock friction: Observations and constitutive equations. *J. Geophys. Res.* 97: 4923-4940.
13. Nakatani, M. and H. Mochizuki. 1996. Effects of shear stress applied to surfaces in stationary contact on rock friction. *Geophys. Res. Lett.* 23: 869-872.
14. Karner, S.L. and C. Marone. 2000. Effects of loading rate and normal stress on stress drop and stick-slip recurrence interval. In *A.G.U. Monograph 120: Geocomplexity and the Physics of Earthquakes*, eds. J.B. Rundle, D.L. Turcotte, W. Klein. American Geophysical Union, Washington DC, 187-198.
15. Ramsey, J.M. and F.M. Chester. 2004. Hybrid fracture and the transition from extension fracture to shear fracture. *Nature* 428: 63-66.
16. Johnson, B., M. Friedman, T.W. Hopkins, and S.J. Bauer. 1987. Strength and microfracturing of Westerly Granite extended wet and dry at temperatures to 800 degrees C and pressures to 200 MPa. In *Proc. of 28th U.S. Symposium on Rock Mechanics*, v. 28, p. 399-412.
17. Brantley, S.L., B. Evans, S.H. Hickman, and D.A. Crerar. 1990. Healing of microcracks in quartz: implications for fluid flow. *Geology* 18: 136-139.
18. Chester, F.M. and N.G. Higgs. 1992. Multimechanism friction constitutive model for ultrafine quartz gouge at hypocentral conditions. *J. Geophys. Res.* 97: 1857-1870.
19. Karner, S.L., C. Marone, and B. Evans. 1997. Laboratory study of fault healing and lithification in simulated fault gouge under hydrothermal conditions. *Tectonophys.* 277: 41-55.

20. Blanpied M.L., C.J. Marone D.A. Lockner, J.D. Byerlee and D.P. King. 1998. Quantitative measure of the variation in fault rheology due to fluid-rock interactions. *J. Geophys. Res.* 103: 9691-9712.

21. Olsen M.P., C.H. Scholz, and A. Léger. 1998. Healing and sealing of a simulated fault gouge under hydrothermal conditions: Implications for fault healing. *J. Geophys. Res.* 103: 7421-7430

22. Tenthorey, E., S.F. Cox, and H.F. Todd. 2003. Evolution of strength recovery and permeability during fluid-rock reaction in experimental fault zones. *Earth Plan. Sci. Lett.* 206: 161-172.

23. Brace, W.F., J.B. Walsh, and W.T. Frangos. 1968. Permeability of granite under high pressure. *J. Geophys. Res.* 73: 2225-2236.

24. Walsh, J.B. and W.F. Brace. 1984. The effect of pressure on the porosity and transport properties of rock. *J. Geophys. Res.* 89: 9425-9431.

25. Moore, D.E., D.A. Lockner, and J.D. Byerlee. 1994. Reduction of permeability in granite at elevated temperatures. *Science* 265: 1558-1561.

26. Oda, M., T. Takemura, and T. Aoki. 2002. Damage growth and permeability change in triaxial compression tests of Inada granite. *Mech. of Mat.* 34: 313-331.

27. Bobich, J.K., F.M. Chester, and J.S. Chester. 2004. Experimental Analysis of Hybrid Fracture in Berea Sands. *Eos Transactions AGU*, 85 (47), Fall Meeting Supplement, Abstract T41F-1297.

28. Jaeger, J.C. and N.G.W. Cook. 1971. *Fundamentals of Rock Mechanics*. Reprint of 1st ed. London: Chapman and Hall Ltd.

29. Heard, H.C., A.E. Abey, B.P. Bonner, and R.N. Schock. 1974. Mechanical behavior of dry Westerly Granite at high pressure. Report 51642: Lawrence Livermore Lab., 14 pp.

30. Logan, J.M. and J. Handin. 1971. Triaxial compression testing at intermediate strain rates. In *Dynamic Rock Mechanics*, 12th Symposium Rock Mechanics AIME, New York, 167 pp.

31. Baria, R., S. Michelet, J. Baumgaertner, B. Dyer, J. Nicholls, T. Hettkamp, D. Teza, N. Soma, H. Asanuma, J. Garnish, T. Megel, T. Kohl, and L. Kueperkoch. 2005. A 5000m deep reservoir development at the European HDR site at Soultz. In *Proc. 30th Workshop Geothermal Reservoir Engineering, Stanford University, Stanford CA, Jan 31-Feb 2 2005*, p. 291-298.

32. Wyborn, D., L. de Graaf, S. Davidson, and S. Hann. 2004. Development of Australia's first hot fractured rock (HFR) underground heat exchanger, Cooper Basin, South Australia. In *Proc. PESA Eastern Australasian Basins Symp. II: Adelaide, 19–22 Sept. 2004*, p. 423-430.

33. Bowden, F.P. and D. Tabor. 1964. *The Friction and Lubrication of Solids. Parts I, II*. Oxford University Press, London.

34. Marone, C. 1998. Laboratory-derived friction laws and their application to seismic faulting. *Annual Review Earth and Planetary Sciences* 26: 643-696.

35. Dieterich, J.H. 1979. Modeling of rock friction: 1. Experimental results and constitutive equations. *J. Geophys. Res.*, 84: 2161-2168.

36. Ruina, A. 1983. Slip instability and state variable friction laws. *J. Geophys. Res.*, 88:10359-10370.

37. Karner, S.L. and C. Marone. 1998. The effect of shear load on frictional healing in simulated fault gouge. *Geophys. Res. Lett.* 25: 4561-4564.

38. Nakatani, M. 1998. A new mechanism of slip-weakening and strength recovery of friction associated with the mechanical consolidation of gouge. *J. Geophys. Res.*, 103: 27239-27256.

39. Karner, S.L., and C. Marone. 2001. Frictional restrengthening in simulated fault gouge: Effect of shear load perturbations. *J. Geophys. Res.*, 106: 19319-19337.

40. Richardson, E., and C. Marone. 1999. Effects of normal stress vibrations on frictional healing, *J. Geophys. Res.*, 104: 28859-28878.

41. Sleep, N.H., E. Richardson, and C. Marone. 2000. Physics of friction and strain rate localization in synthetic fault gouge. *J. Geophys. Res.*, 105: 25875-25890.

42. Karner, S.L., F.M. Chester, and J.S Chester. 2004. Towards a General State-variable Constitutive Relation to Describe Granular Deformation. *Earth Planet. Sci. Lett.* 237: 940-950.

43. Karner, S.L. 2006. An extension of rate and state theory to poromechanics, *Geophys. Res. Lett.* 33: L03308, doi:10.1029/2005GL024934.

44. Karner, S.L. and B.C. Schreiber. 1993. Experimental Simulation of Plagioclase Diagenesis at P-T Conditions of 3.5km Burial Depth. *Pure Appl. Geophys.* 141: 221-247.

45. Reinen, L.A. and J.D. Weeks, 1993. Determination of rock friction constitutive parameters using an iterative least-squares inversion method, *J. Geophys. Res.* 98, 15937-15950.